Steinert, P. M., Steven, A. C., & Roop, D. R. (1985a) *Cell (Cambridge, Mass.) 42*, 411-420.
Steinert, P. M., Parry, D. A. D., Idler, W. W., Johnson, L. D., Steven, A. C., & Roop, D. R. (1985b) *J. Biol. Chem. 260*, 7142-7149.
Steven, A. C., Hainfeld, J. F., Trus, B. L., Wall, J. S., & Steinert, P. M. (1983) *J. Cell Biol. 97*, 1939-1944.
Steven, A. C., Trus, B. L., Hainfeld, J. F., Wall, J. S., & Steinert, P. M. (1985) *Ann. N.Y. Acad. Sci. 455*, 371-379.
Torchia, D. A. (1984) *Annu. Rev. Biophys. Bioeng. 13*, 125-144.
Torchia, D. A., & Piez, K. A. (1973) *J. Mol. Biol. 76*, 419-424.
Torchia, D. A., Batchelder, L. S., Fleming, W. W., Jelinski, L. W., Sarkar, S. K., & Sullivan, C. E. (1983) *Ciba Found. Symp. 93*, 98-111.
Wittebort, R. J., Olejniczak, E. T., & Griffin, R. G. (1987) *J. Chem. Phys. 86*, 5411-5420.

Tyrosine Hydrogen-Bonding and Environmental Effects in Proteins Probed by Ultraviolet Resonance Raman Spectroscopy†

Peter G. Hildebrandt,‡ Robert A. Copeland,§ and Thomas G. Spiro*
Department of Chemistry, Princeton University, Princeton, New Jersey 08544
Jacek Otlewski‖ and Michael Laskowski, Jr.
Department of Chemistry, Purdue University, West Lafayette, Indiana 47907
Franklyn G. Prendergast
Department of Biochemistry and Molecular Biology, Mayo Foundation, Rochester, Minnesota 55901
Received December 30, 1987; Revised Manuscript Received March 14, 1988

ABSTRACT: Ultraviolet resonance Raman spectra with 229-nm excitation are reported for aqueous tyrosine and for ovomucoid third domain proteins from chicken [OMCHI3(-)] and from chachalaca [OMCHA(-)], as well as α_1-, α_2-, and β-purothionin. At this excitation wavelength interference from phenylalanine is minimized, and it is possible to determine the frequencies of the Tyr ring modes ν_{8a} and ν_{8b}. The ν_{8b} frequency decreases with the degree of Tyr H-bond donation, reaching a limiting value for deprotonated tyrosine. This spectroscopic indicator of H-bond strength was calibrated by using the model compound *p*-cresol in H-bond acceptor solutions for which the enthalpy of H-bond formation can be obtained from the literature. With this calibration it is possible to estimate Tyr H-bond enthalpies in proteins for which Tyr is a H-bond donor; values of 13.7, 9.6, and 11.2 kcal/mol were found for OMCHA3(-) and for α_1- (or α_2-) and β-purothionin, respectively. The intensity of the 1176-cm^{-1} ν_{9a} band of Tyr excited at 229 nm and also the intensity ratio of the Tyr 830/850-cm^{-1} Fermi doublet excited at 200 nm both correlate strongly with the estimated H-bond enthalpies, but large deviations are seen for the purothionins, reflecting a special environment for the Tyr residue of these proteins, which is believed to be constrained in a hydrophobic pocket. The molar intensity of the strong $\sim$1000-cm^{-1} ν_{12} band of phenylalanine in aqueous solution is about half the value observed in most proteins. Addition of ethylene glycol to aqueous phenylalanine increases the intensity, which attains a value similar to those seen in proteins. Protein environmental effects on UVRR intensities for aromatics are expected to be common.

The importance of hydrogen bonding (H-bonding)[1] in protein structure and reactivity is well established (Creighton, 1983). Amide backbone H-bonding is the key structural element determining secondary structures of proteins. The H-bonding of individual amino acid side chains to other residues and to substrates plays important roles in enzyme mechanisms (Cantor & Schimmel, 1980a; Walsh, 1979). Among the amino acid side chains that can participate in H-bonding, the phenolic hydroxide of tyrosine (Tyr) can serve as either proton donor or acceptor, or both simultaneously (Baker & Hubbard, 1984). For this reason biochemists have long sought spectroscopic probes of tyrosine H-bonding in proteins.

The most widely used method for studying Tyr phenolic H-bonding is ultraviolet (UV) (difference) absorption spectroscopy (Demchenko, 1986; Cantor & Schimmel, 1980b). However, this approach requires one to differentiate the effect of Tyr hydrogen bonding from all the possible interactions of the chromophore in the protein matrix. Fluorescence spectroscopy (Demchenko, 1986) may also be employed but is

† This work was supported at Princeton by NIH Grant GM 25158 to T.G.S. and at Purdue by NIH Grant GM 10831 to M.L.
* Author to whom correspondence should be addressed.
‡ Present address: Max-Planck-Institut für biophysikalische Chemie, Abteilung Spektroskopie, D-3400 Göttingen, FRG.
§ Present address: Arthur Amos Noyes Laboratory of Chemical Physics, 127-72, California Institute of Technology, Pasadena, CA 91125.
‖ Present address: Institute of Biochemistry, University of Wroclaw, Tamka 2, 50-137 Wroclaw, Poland.

[1] Abbreviations: UVRR, ultraviolet resonance Raman; H-bond, hydrogen bond; Tyr, tyrosine; Trp, tryptophan; Phe, phenylalanine; OHMCHA3(-), chachalaca ovomucoid third domain carbohydrate free; OMCHI3(-), chicken ovomucoid third domain carbohydrate free; Erb, erabutoxin B; Pα_1, Pα_2,Pβ, purothionin α_1, α_2, β; S/N, signal to noise ratio; Asp, aspartate.

0006-2960/88/0427-5426$01.50/0

usually practicable only in the absence of tryptophan (Trp) due to the much stronger and overlapping fluorescence of the indole chromophore and the common occurrence of Tyr → Trp resonance energy transfer. Nonresonant Raman spectroscopy (Tu, 1986) has been applied to estimate the number of hydrogen-bonded and solvent-exposed Tyr residues on the basis of the intensity ratio of the 830/850-cm^{-1} Fermi doublet. The main disadvantage of this technique is the requirement for high protein concentrations and the low relative intensities of these marker bands.

Recently, UV resonance Raman (UVRR) spectroscopy has been shown to be a powerful technique for elucidating the structure of proteins (Johnson et al., 1984; Chinsky et al., 1985; Rava & Spiro, 1984, 1985a,b; Copeland & Spiro, 1985, 1986, 1987; Asher et al., 1986; Hudson & Mayne, 1984). Selective enhancement of the Raman bands of the amide bond and of the aromatic amino acid residues is possible with appropriate choice of excitation wavelength. In the present study we have employed this technique to probe the vibrational spectrum of Tyr and its sensitivity to hydrogen-bond donation. In order to make full use of the information obtained from UVRR spectra, it was necessary initially to study systems where the environment of Tyr is well-defined. For this purpose we have examined small proteins—carbohydrate-free ovomucoid third domain from chicken [OMCHI3(−)] and chachalaca [OMCHA3(−)] (Laslowski et al., 1987) and erabutoxin b (Erb) (Harada et al., 1976)—in which the Tyr residues are either strongly or weakly hydrogen-bonded. In addition, because the vibrational patterns of Tyr and *p*-cresol are similar, it was possible to use *p*-cresol as a model compound. Thus, the investigations could be extended to H-donor/acceptor complexes in an inert solvent for which the strength of the H-bond can be expressed in terms of the enthalpy of formation, ΔH. The main goal here was to derive quantitative correlations between the spectral and the thermodynamic parameters.

This goal has been accomplished via measurement of the frequency of the Tyr ring mode ν_{8b}, which is shown to depend linearly on the H-bond enthalpy when Tyr is a H-bond donor. Thus, the determination of ν_{8b}, which is optimally enhanced, relative to interfering protein residues, via excitation at 229 nm, can be used to gauge the strength of the Tyr donor H-bonds. Other indices of H-bonding interaction have also been evaluated, including the UVRR intensity ratio of the Tyr Fermi doublet and the intensity of the ring mode ν_{9a}. In both cases sensitivity to H-bonding is demonstrated, but quantitative evaluation is complicated by other environmental influences. An interesting illustration of multiple influences on the UVRR markers is provided by the purothionin plant toxins, for which previous attempts to gauge Tyr H-bonding (nonresonant Raman, fluorescence) have given contradictory results (Prendergast et al., 1984). The sensitivity of UVRR intensities to environmental effects is underscored by measurement of the ν_{12} ring mode intensity of phenylalanine, which is shown to nearly double when the solvent is changed from water to 80% ethylene glycol; this higher cross section is in the range observed for several proteins, the enhancement being attributable to hydrophobic environments.

Experimental Procedures

Erabutoxin b (Erb) from *Laticauda semifasciata* was purchased from Sigma and used without further purification. Ovomucoid third domains in their carbohydrate-free form were isolated from egg white of chicken [OMCHI3(−)] and plain chacalaca [OMCHA3(−)] as described elsewhere (Laskowski et al., 1987; Kato et al., 1987). α_1-, α_2-, and β-purothionins were prepared as described previously (Prendergast et al., 1984; Lecomte et al., 1982). The lyophilized proteins were dissolved in aqueous 0.05 M phosphate buffer (pH as indicated) to a concentration of ~2 and ~7 mg/mL for RR spectra at 200- and 229-nm excitation, respectively.

Adjustments of the pH, which was determined with a Corning Model 150 pH meter, were made with small volumes of aqueous HCl or NaOH. Some samples additionally contained sodium sulfate (0.4 M) or sodium perchlorate (0.3 M) as internal standards. All chemicals were of the highest purity grade. UVRR spectra were obtained with 200- and 229-nm excitation as described elsewhere (Fodor et al., 1986). The spectra were recorded with 0.05 Å/s increments. Raman scattering was collected from a flowing stream of sample solution. The S/N ratio was improved by repetitive scanning (10–30 scans). No time-dependent changes were noted from scan to scan, indicating the stability of the sample in the UV laser beam. Also, UV absorption spectra (Hewlett-Packard 8450 A diode array UV–vis spectrophotometer), taken after Raman data acquisition, showed no evidence of laser-induced damage for any of the samples. Visible Raman spectra were obtained with the 514.5-nm argon laser line by using conventional Raman equipment (Walters et al., 1983).

Absolute Raman cross sections were determined by comparing the band intensities with the totally symmetric stretching vibration of sulfate or perchlorate. The reference cross section for sulfate was adopted from Fodor et al. (1987); the corresponding value for perchlorate at 229 nm was determined via the relative intensities in a SO_4^- aqueous mixture to be 0.519 mbarn/molecule × str (number of stretching vibrations).

Results and Discussion

(A) ν_{8b} Frequency and Tyrosine H-Bond Strength. The highest frequency ring modes of substituted benzenes, which are found in the region of 1600 cm^{-1}, are labeled ν_{8a} and ν_{8b}, signifying their parentage in the doubly degenerate mode ν_8 of unsubstituted benzene (Dolish et al., 1974). For monosubstituted or para-disubstituted benzenes the subscripts a and b identify modes that are symmetric and antisymmetric, respectively, with respect to the twofold molecular rotation axis. The frequencies of these modes depend on the nature of the substituents, and the antisymmetric ν_{8b} mode is particularly sensitive. In tyrosine, ν_{8a} and ν_{8b} are found at 1616 and 1600 cm^{-1}, respectively, but in D_2O, ν_{8b} shifts to 1587 cm^{-1} (Copeland & Spiro, 1985). This shift reflects the coupling of the O–H bending coordinate with the antisymmetric ν_{8b}; when H is replaced by D, this coupling is relieved, since the natural frequency for O–D bending is much lower than for O–H bending. When the O–H is deprotonated, the coupling is likewise relieved, and in addition the charge redistribution in tyrosinate shifts ν_{8b} still further down, to 1555 cm^{-1} (Dolish et al., 1974).

The ν_{8a} and ν_{8b} modes of tyrosine are strongly enhanced in UVRR spectra (Fodor et al., 1987). Because of the large ν_{8b} downshift upon deprotonation, it has been recognized that its frequency might be sensitive to H-bonding in proteins (Copeland & Spiro, 1985). Indeed, changes in the ~1600-cm^{-1} region of the UVRR spectra of methemoglobin fluoride between R and T states were interpreted in these terms (Copeland et al., 1985). Unfortunately, the issue was obscured by interference from the phenylalanine (Phe) ν_{8a} and ν_{8b} modes that fall in the same region (1607 and 1588 cm^{-1}). Since Phe occurs in nearly all proteins, this interference is a quite general problem.

Recent measurements of excitation profiles for Tyr and Phe (Fodor et al., 1987) reveal that the problem becomes man-

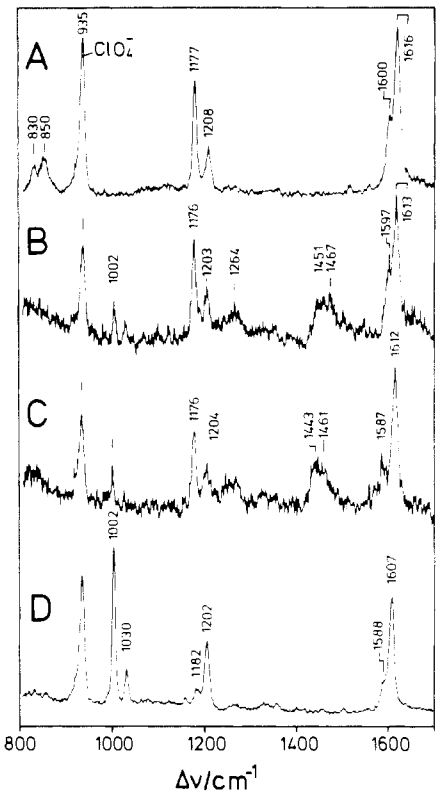

FIGURE 1: Raman spectra excited at 229 nm: (A) tyrosine, 2 mM, in 1 M $NaClO_4$, pH 7.0; (B) OMCHA3(−), 1.2 mM, in 0.3 M $NaClO_4$, pH 1.5; (C) OMCHA3(−), 1.2 mM, in 0.3 M $NaClO_4$, pH 7.0; (D) phenylalanine, 50 mM, in 1 M $NaClO_4$, pH 7.0.

ageable if the UV excitation wavelength is 229 instead of 200 nm. The latter wavelength was used in earlier UVRR protein studies (Rava & Spiro, 1984, 1985; Copeland et al., 1985) in order to enhance peptide as well as aromatic contributions, while minimizing interference from Trp, whose optimal excitation wavelength is 218 nm (Rava & Spiro, 1985b; Fodor et al., 1987). For both tyrosine and phenylalanine, ν_{8a} and ν_{8b} are strongly enhanced in resonance with the quasi-forbidden L_a transition via vibronic coupling with the allowed $B_{a,b}$ transitions (Ziegler & Hudson, 1981, 1983; Fodor et al., 1987). The L_a transition of Phe is blue-shifted relative to that of Tyr, so that at 229 nm the Phe enhancement is quite low, while that of Tyr remains high. The Tyr/Phe enhancement ratio for ν_{8a} at 229 nm is ~30 (Fodor et al., 1987), so that Phe interference at this wavelength is expected to be minimal. This is borne out by the UVRR spectra at 229-nm excitation shown in Figure 1. The top and bottom spectra are of aqueous Tyr and Phe, respectively [see Rava and Spiro (1985b) for band assignments], while spectra B and C are of the OMCHA3(−) at pH 1.5 and pH 7, respectively. This protein (Laskowski et al., 1987) contains three Phe and one Tyr residues, but the Phe contribution to the 229-nm UVRR spectra is quite small, as can be seen from the magnitude of the 1002-cm^{-1} band, which is the strongest band in the Phe spectrum. The contribution of the ν_{8a} and ν_{8b} Phe bands is expected to be ~10% of the Tyr contribution. The remaining protein bands are due to Tyr (1176, 1203 cm^{-1}), amide III (1264 cm^{-1}), and CH_2 deformation modes (~1450 cm^{-1}) (Rava & Spiro, 1984, 1985a; Copeland & Spiro, 1985).

The ovomucoid proteins are strong serine protease inhibitors (Laskowski & Kato, 1980). Crystal structures of the third domain have been determined for three representatives of this family [Japanese quail (Weber et al., 1981; Papamokos et al., 1982), turkey (Read et al., 1983), and silver pheasant (Bode et al., 1985)]. In all cases, Tyr^{31} donates an H-bond to the carboxylate of Asp^{27}. This is an important structural feature as Tyr^{31} is completely conserved in all 101 avian species studied; Asp^{27} is conserved in 100 of these. At pH 1.5, the Asp^{27} residue is protonated and the interaction with the Tyr^{31} residue is greatly weakened or abolished (Laskowski et al., 1987). The effect of this change is seen clearly in the UVRR spectra of OMCHA3(−) (Figure 1), which contains only the H-bonded Tyr^{31} (Laskowski et al., 1987). At pH 1.5 the ring modes ν_{8a} and ν_{8b} are found at 1613 and 1597 cm^{-1}, close to the values observed for aqueous tyrosine (Figure 1). At pH 7.0 the frequencies are 1612 and 1587 cm^{-1}. The strong Tyr^{31}–Asp^{27} H-bond is clearly reflected in the 10-cm^{-1} downshift of ν_{8b}.

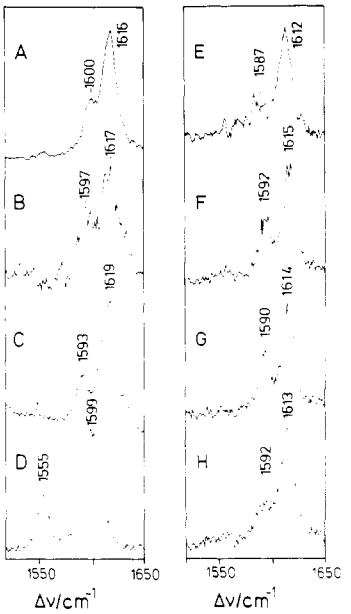

FIGURE 2: Raman spectra of tyrosine, *p*-cresol, and several proteins in the ν_{8a}/ν_{8b} region. The spectra were excited at 229 nm except for (C), which was excited at 514.5 nm: (A) Tyr, aqueous solution, pH 7.0; (B) *p*-cresol/*n*-butyl ether/cyclohexane; (C) *p*-cresol/triethylamine; (D) Tyr^-, aqueous solution, pH 12.5; (E) OMCHA3(−), aqueous solution, pH 7.0; (F) α_1-purothionin, aqueous solution, pH 7.0; (G) β-purothionin, aqueous solution, pH 7.0; (H) OMCHI3(−), aqueous solution, pH 7.0. For concentrations see Table I.

Figure 2 illustrates the systematics of the H-bond effect on the ν_{8a} and ν_{8b} bands, which are shown on an expanded scale for proteins and model systems. We chose *p*-cresol as a model since the substitution of CH_3 for the CH_2 group of tyrosine leaves the chromophore vibrational modes essentially unaltered and *p*-cresol can be dissolved in solvents having variable H-bond acceptor propensities. A steady increase in ν_{8b} is seen when tyrosinate (spectrum D) is compared with *p*-cresol in successively weaker H-bond acceptors: triethylamine (C), *n*-butyl ether [2.1 M in cyclohexane (B)], and water (A), in which *p*-cresol has the same UVRR spectrum as tyrosine; *p*-cresol in acetone (1.5 M in cyclohexane) and in cyclohexane (spectra not shown) gives ν_{8b} = 1598 and 1604 cm^{-1} (Table I). The *p*-cresol concentration (2 mM) was low enough that self-association was negligible (Fritzsche, 1964), so the spectrum in cyclohexane can be taken as the base line with no H-bonding. The remaining *p*-cresol spectra can serve to define a H-bond function from thermodynamic data available from the literature (Arnett et al., 1970; Joesten & Schaad, 1974; Sherry, 1976; Singh et al., 1966; Thijs & Zeegers-Huyskens, 1984; Joesten & Drago, 1962; Eploy & Drago, 1967; Vogel & Drago, 1970; Gramstad, 1961, 1963; Dunken & Fritzsche, 1961; Neerinck et al., 1969; Singh & Rao, 1966;

Table I: ν_{8a} and ν_{8b} Frequencies (cm^{-1}) for *p*-Cresol and Tyrosine in Media of Different H-Bond Acceptor Strengths[a]

system[b]	ν_{8a}	ν_{8b}	$-\Delta H$[c] (kJ/mol)
p-cresol/cyclohexane	1616	1604	0.0
p-cresol/H_2O	1616	1600	
Tyr/H_2O	1616	1600	
glycyltyrosine/H_2O	1615	1600	
p-cresol/acetone/cyclohexane	1616	1598	4.3
p-cresol/*n*-butyl ether/cyclohexane	1617	1597	5.5
p-cresol/triethylamine	1619	1593	8.8
Tyr^- (pH 12.5)	1599	1555	

[a] Raman spectra probed at 229 nm except for *p*-cresol/H_2O, glycyltyrosine/H_2O, and *p*-cresol/triethylamine (514.5 nm). [b] *p*-Cresol and tyrosine concentrations were 2 mM for the 229-nm spectra and 10 mM for the 514-nm spectra. The concentrations for acetone and *n*-butyl ether were 1.5 and 2.1 M, respectively, so that the complex formation was ≥95% (Thijs & Zeegers-Huyskens, 1984; Joesten & Drago, 1962; Gramstad, 1963; Dunken & Fritzsche, 1961; Neerinck et al., 1969; Singh & Rao, 1966; West et al., 1964; Vogel & Drago, 1970). [c] The ΔH values were obtained from the literature as discussed in the text.

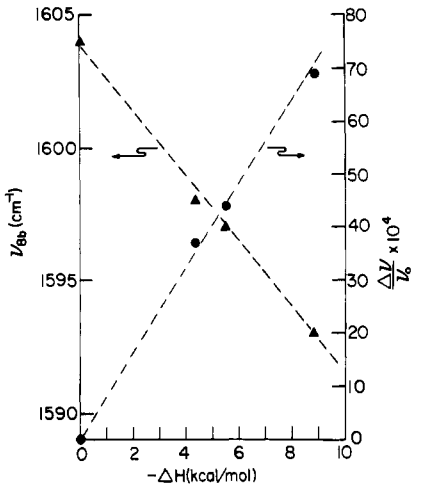

FIGURE 3: Plot of the ν_{8b} frequency and of $\Delta\nu_{8b}/\nu_{8b_0}$ against the enthalpy of the hydrogen-bond formation for *p*-cresol in different solvents; see text and Table I for details.

West et al., 1964; Zharkov et al., 1970; Kogowski et al., 1980; Farak et al., 1979). Enthalpies have been determined for phenol and *p*-cresol with acetone and *n*-butyl ether diluted in CCl_4 and for phenol with the same acceptors diluted in cyclohexane. The enthalpies are slightly smaller in cyclohexane than in CCl_4 (for phenol) and slightly smaller for phenol than for *p*-cresol (in CCl_4) (Thijs & Zeegers-Huyskens, 1984; Joesten & Drago, 1962; Gramstad, 1963; Dunken & Fritzsche, 1961; Neerinck et al., 1969; Singh & Rao, 1966; West et al., 1964; Vogel & Drago, 1970). We assume that these small (~0.5 kcal/mol) compensating differences lead to similar enthalpies for *p*-cresol in cyclohexane, which has not been studied directly, as for phenol in CCl_4, values for which are listed in Table I. In the case of triethylamine as H-bond acceptor, there seem to be more significant differences among different solvents (Fritzsche, 1964; Singh & Rao, 1966; Gramstad, 1961; Zharkov et al., 1970; Eploy & Drago, 1967; Kogowski et al., 1980; Farak et al., 1979). Consequently, we used pure triethylamine for the *p*-cresol spectral measurement and assumed the enthalpy was the same as for phenol in pure triethylamine (Arnett et al., 1970) (Table I).

In Figure 3 we see that ν_{8b} is linearly related to these enthalpy values. The relationship is

$$\nu_{8b}\ (cm^{-1}) = 1603.8 - 1.25\ (-\Delta H) \qquad (1)$$

from a least-squares fit of the four points. A plot of $\Delta\nu_{8b}/\nu_{8b_0}$, where $\Delta\nu_{8b}$ is the ν_{8b} shift relative to the eq 1 intercept, ν_{8b_0}, is also linear; similar relationships have been observed for the phenol O–H stretching frequency, measured in infrared spectra (Sherry, 1976; Singh et al., 1966).

Equation 1 can be used to estimate H-bond strengths for tyrosine from the ν_{8b} frequencies. Thus, the 1600- and 1587-cm^{-1} frequencies observed for aqueous tyrosine and for OMCHA3(−) at pH 7 translate to $-\Delta H$ values of 2.9 and 13.7 kcal/mol, respectively. The latter value requires an extrapolation of eq 1 well beyond the range of available calibration points (0–9 kcal/mol), and we cannot be sure that the relationship is linear in this region. Nevertheless, the ΔH ratio of OMCHA3(−) to aqueous tyrosine is in qualitative accord with the expectation from theoretical calculations that H-bonds to anionic acceptors are 3–4 times stronger than those to neutral acceptors (Weiner et al., 1984; L. C. Allen, private communication). The 13.7 kcal/mol estimate for OMCHA3(−) is much larger than the H-bond energies, in the 3–6 kcal/mol range, to which biochemists are accustomed. These values come from estimates of the H-bond contributions to the free energy of substrate binding to proteins, for example, and they reflect the leveling effect of water as a solvent (Fersht et al., 1985). Binding reactions in water always involve hydrated reactants and products so that one set of H-bonds is being exchanged for another. A spectroscopic indicator like the ν_{8b} frequency, however, reflects the intrinsic strength of the H-bond in the species being monitored. Consequently, H-bond enthalpies in non-H-bonding solvents provide a more appropriate scale than aqueous values for the spectroscopic correlation with H-bond strength. Even for non-H-bonding solvents it is not clear that solvation effects for reactants and products cancel, since theoretical calculations of H-bond energies in vacuum seem to give numbers substantially higher than the nonaqueous enthalpies (e.g., the phenol–H_2O H-bond strength is estimated to be 6.1 kcal/mol; Weiner et al., 1984). For the time being, however, we propose eq 1 as a reasonable calibration of tyrosine donor H-bond strengths.

In the case of OMCHI3(−) there is an additional Tyr (Tyr-11) whose hydroxyl group is exposed to solvent (see previously cited X-ray data). The two ν_{8b} bands cannot be resolved, however, appearing as a single broad envelope centered at 1592 cm^{-1} (spectrum H), which is the average of the aqueous Tyr and OMCHA3(−) frequencies. At pH 1.5, where the Asp carboxylate group is protonated, OMCHA3(−) and OMCHI3(−) both show ν_{8b} at 1597 cm^{-1}, nearly the same as aqueous Tyr (1600 cm^{-1}). The 3-cm^{-1} difference is probably real, however, and may reflect a residual H-bond interaction, since the proteins retain their tertiary structure at low pH (Laskowski et al., 1987).

Spectra F and G are of α_1- and β-purothionins ($P\alpha_1$ and $P\beta$) and reveal strong H-bonds, with ν_{8b} at 1592 and 1590 cm^{-1}, respectively, corresponding to $-\Delta H$ = 9.6 and 11.2 kcal/mol via eq 1. $P\alpha_2$ (not shown) gives a spectrum indistinguishable from that of $P\alpha_1$. The purothionins are small (~5 kDa) plant toxins that contain a single tyrosine residue (Tyr-13) (Mak, 1975; Mak & Jones, 1976; Jones & Mak, 1977). Their primary sequences are similar to that of crambin, another plant toxin, for which a high-resolution X-ray structure is available (Hendrickson & Teeter, 1981; Teeter & Hendrickson, 1979). The secondary structure of these proteins has been shown by visible Raman spectroscopy (Williams & Teeter, 1984) to be quite similar. They lack tryptophan, and their tyrosine fluorescence spectra have been studied (Prendergast et al., 1984). Crambin shows a typical Tyr fluorescence spectrum with maximum emission at ~305 nm, but $P\alpha_1$ and $P\alpha_2$ give a double-humped spectrum with maxima at 308

Table II: Tyrosine H-Bond UVRR Markers and the Phenylalanine ν_{12} Cross Section for the Proteins in This Study

		Tyr				Phe
	pH	ν_{8b} (cm^{-1})	$-\Delta H_{est}$[a] (kcal/mol)	R_{200}[b]	$\sigma^{229}_{\nu_{9a}}$[c] (mbarn/molecule × str)	$\sigma^{229}_{\nu_{12}}$[d] (mbarn/molecule × str)
tyrosine	7.0	1600	3.0	0.34	167	
tyrosinate	12.5	1555		0.77	80	
Erb	7.0	*e*		1.1	*e*	*e*
Erb	1.5	*e*		0.34	*e*	*e*
OMCHA3(−)	7.0	1587	13.7	1.0	111	21[g]
OMCHA3(−)	1.5	1597	5.5	0.52	147	21[g]
OMCHI3(−)	7.0	1592[f]	9.6[f]	0.71[f]	122[f]	*e*
OMCHI3(−)	1.5	1597[f]	5.5[f]	0.43[f]	152[f]	*e*
Pα_1	7.0	1592	9.6	0.42	80	27
Pα_2	7.0	1592	9.6	*e*	90	24
Pβ	7.0	1590	11.2	0.62	*e*	*e*
phenylalanine	7.0					13

[a] Tyr H-bond enthalpy estimated from the ν_{8b} frequency via eq 1. [b] Fermi doublet intensity ratio, I_{830}/I_{850}, measured at 200 nm. [c] Tyr ν_{9a} (1177 cm^{-1}) cross section measured at 229 nm. [d] Phe ν_{12} (1002 cm^{-1}) cross section measured at 200 nm. [e] Not recorded. [f] Average value for two Tyr residues. [g] Average value for three Phe residues.

and 345 nm, while Pβ shows a single maximum at 345 nm. In the absence of tryptophan residues, an emission maximum at 345 nm is associated with tyrosine ionization, which can in principle occur either in the ground or in the excited state. On the basis of pH–titration data it was concluded (Prendergast et al., 1984) that the purothionin 345-nm emission was attributable to excited-state, rather than ground-state tyrosine ionization. The UVRR spectra (Figure 2) confirm that the purothionins contain no significant amount of ground-state tyrosinate, which would show ν_{8a} and ν_{8b} bands at 1599 and 1555 cm^{-1}. Excited-state ionization presumably occurs along the pathway provided by the strong ground-state H-bond. The stronger H-bond detected for Pβ compared to that for Pα_1 and Pα_2 might account for the greater fraction of 345-nm emission. However, not all proteins with Tyr H-bonds show the 345-nm emission, and other factors in the Tyr environment may play an important role (see below).

We note that there are slight differences among the Tyr ν_{8a} frequencies in the proteins and models examined here, but there is no systematic variation with H-bond strength (Table I). The protein variations may reflect residual contributions from the Phe ν_{8a} band.

(B) Tyrosine Fermi Doublet. The tyrosine residue shows a characteristic doublet at 830/850 cm^{-1}, whose variable intensity is known to depend on hydrogen bonding. This doublet results from a Fermi resonance between the ring breathing mode, ν_1, and the overtone of an out-of-plane ring deformation, ν_{16a}. Siamwiza et al. (1975) carried out an extensive study of tyrosine model compounds and established an empirical correlation between the intensity ratio, $R = I_{830}/I_{850}$, and the H-bond state of the phenolic OH group. With excitation at visible wavelengths the ratio is ~2.0 for strongly H-bonded Tyr, while a value of ~0.77 is characteristic for solvent-exposed Tyr. The Fermi doublet is enhanced with UV excitation at 200 nm, and a similar H-bond trend has been suggested (Rava & Spiro, 1985b), although the intensity ratios are quantitatively different from those measured with visible excitation, presumably reflecting different resonance enhancement factors for ν_1 and $2\nu_{16a}$. McHale (1982) has shown how R depends on the coupling strength between the two modes, their polarizabilities, and the frequency difference between them. Any or all of these parameters could be affected by H-bonding.

Figure 4 shows 200-nm-excited RR spectra for the snake venom toxin erabutoxin b (Erb) at pH 1.5 (A) and pH 7 (B). At this wavelength amide modes, as well as those of aromatic residues, are enhanced. The amide I, II, and III bands at

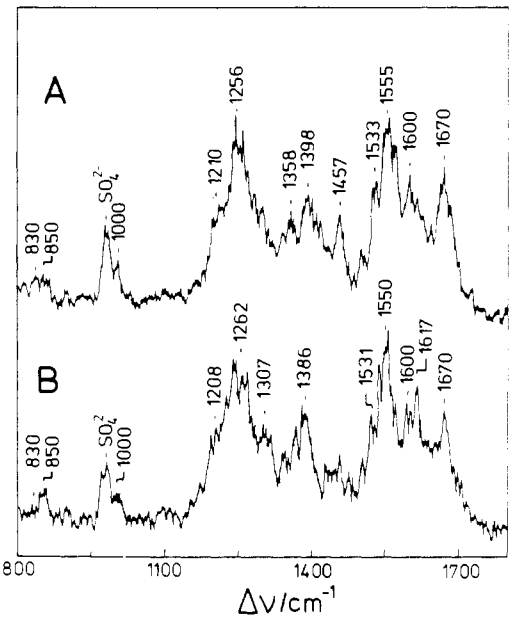

FIGURE 4: Raman spectra of erabutoxin (2 mg/mL) in aqueous solution at pH 7.0 (A) and pH 1.5 (B) excited at 200 nm. The sulfate concentration was 0.4 M.

~1670, 1555, and 1260 cm^{-1} are seen prominently. The intensity ratio of amide II to amide I increases upon acidification, implying a decrease in the α-helical structure (Copeland & Spiro, 1986). Attention is drawn to the 830/850-cm^{-1} Fermi doublet, which is shown in greater detail in Figure 5. The intensity ratio, measured with 200-nm excitation, $R_{200} = I_{830}/I_{850}$, has the same value at pH 1.5 as does aqueous tyrosine, 0.34, while the value for Erb at pH 7.0 is much larger, 1.0. Comparison with a nearby ν_1 band of sulfate ion, added as an internal standard, shows that the change is due to a lowering of the 850-cm^{-1} component at the higher pH, presumably due to a lower enhancement factor for the ring ν_1 mode. The single Tyr residue is H-bonded in the native state but not at low pH (Harada et al., 1976) as in the case of OMCHA3(−). The latter protein likewise shows a decrease in R_{200}, from 1.0 at pH 7 to 0.52 at pH 1.5 (see Table II). In OMCHI3(−), which has both a strongly H-bonded and a solvent-exposed Tyr, R_{200} = 0.71, close to the average for weakly and strongly H-bonded Tyr; a decrease, to 0.43, is again seen at pH 1.5. The R_{200} values for both OMCHA(−) and OMCHI3(−) at pH 1.5 are slightly but noticeably larger than for aqueous tyrosine. Thus, both ν_{8b} and R_{200} suggest

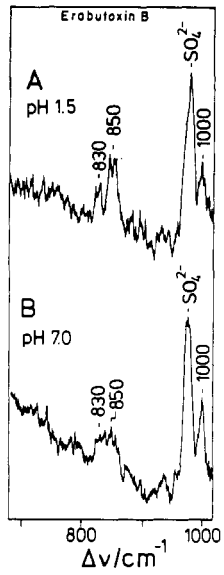

FIGURE 5: Raman spectra of erabutoxin in the Fermi doublet region, with 200-nm excitation: (A) pH 1.5; (B) pH 7.0. Concentrations as in Figure 3.

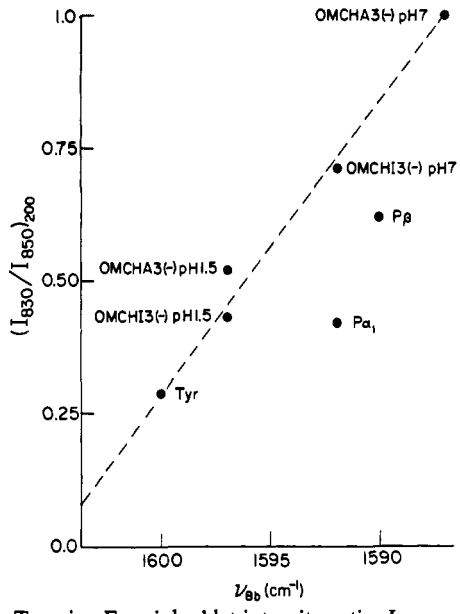

FIGURE 6: Tyrosine Fermi doublet intensity ratio, $I_{830/850}$, measured with 200-nm excitation plotted against ν_{8b} for tyrosine and several proteins, as indicated. Large negative deviations are seen for α_1- and β-purothionin (see text).

that the Tyr residues are not completely solvated in the unfolded proteins.

Figure 6 shows a good correlation between R_{200} and the ν_{8b} frequency for Tyr and the ovomucoid proteins. The relationship is

$$R_{200} = 0.140 + 0.050\Delta\nu_{8b} \quad (2)$$

where $\Delta\nu_{8b} = 1603.8 - \nu_{8b}$. Large negative deviations are seen, however, for the purothionins. We tentatively ascribe these deviant values to environmental effects. On the basis of sequence similarities of the purothionins with crambin it is assumed that the Tyr residue is enclosed in a tight slot in the protein (Prendergast et al., 1984). It may be that the resulting hydrophobic environment increases the 850-cm^{-1} band enhancement, counteracting the effect of the strong H-bond.

(*C*) *Tyrosine ν_{9a} Intensity*. Examination of Figure 1 shows that acidification of OMCHA3(−) leads to intensity augmentation of the 1176-cm^{-1} band. This band arises from ring mode ν_{9a}, which along with ν_{8a}/ν_{8b} gains its intensity via the

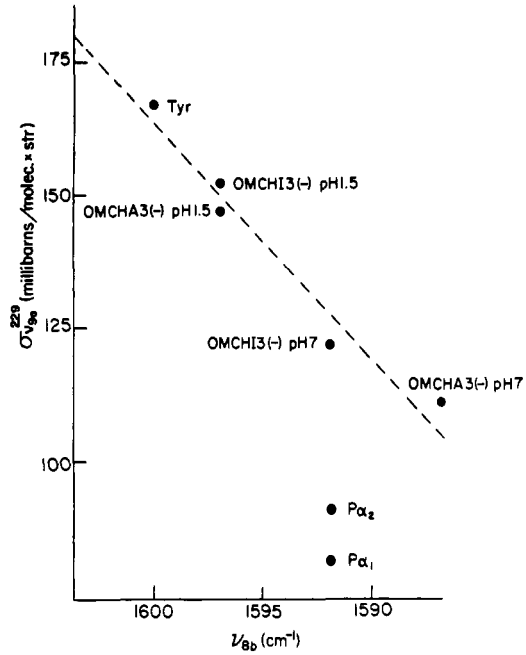

FIGURE 7: Raman cross section for Tyr mode ν_{9a} plotted against ν_{8b}. The deviant values are for α_1- and α_2-purothionin.

vibronic mechanism (Rava & Spiro, 1985b). The ν_{9a} cross section was measured for tyrosine and for several of the protein samples and is given in Table II. Figure 7 shows that there is a strong negative correlation between $\sigma^{229}_{\nu_{9a}}$ and $\Delta\nu_{8b}$:

$$\sigma^{229}_{\nu_{9a}} \text{ (mbarn/molecule} \times \text{str)} = 180 - 4.32\Delta\nu_{8b} \quad (3)$$

The simplest explanation of this trend is that the resonant L_a absorption band (Fodor et al., 1987) shifts to the red upon Tyr H-bond donation, thereby reducing the resonance enhancement at 229 nm. Consistent with this interpretation, the ν_{9a} cross section is 50% lower for tyrosinate than for tyrosine; deprotonation produces a large red shift of the L_a absorption band.

Again the purothionins give strong negative deviations from the correlation, reinforcing the evidence from the Fermi doublet measurements that the Tyr residue is in a special environment that perturbs the intensities.

(*D*) *Phenylalanine ν_{12} Intensity*. In order to assess further the environmental sensitivity of aromatic ring mode UVRR intensities, we measured the cross section of the strong ν_{12} phenylalanine band at ~1000 cm^{-1}. These are also listed in Table II. The protein values [which for OMCHA3(−) represent an average over three Phe residues] show a substantial range of variation and are roughly twice as large as for aqueous Phe.

Since the Phe residue cannot undergo specific H-bond or other polar interactions, the variations in $\sigma_{\nu_{12}}$ must arise from environmental influences on the benzene ring π electron cloud. The L_a absorption band of Phe is known (Donovan, 1973) to intensify and shift to the red in hydrophobic environments. This electronic effect could readily account for the higher values of $\sigma_{\nu_{12}}$ seen in the proteins than in aqueous Phe. Figure 8 provides confirmation at this hypothesis. Ethylene glycol, which has been used (Donovan, 1973) to model the environment of Phe in proteins, produces a marked intensification of ν_{12} when added to an aqueous Phe solution. The cross section levels off at a value, 23 mbarn/molecule × str, that is in the range observed for the proteins.

These measurements establish that there are significant environmental effects on aromatic ring mode intensities in proteins, which will have to be taken into account in interpreting UVRR intensity data.

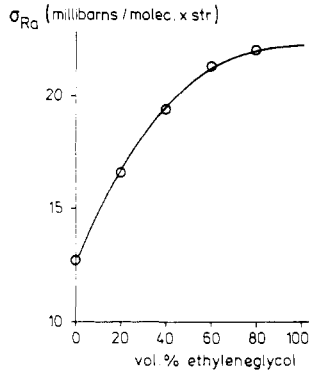

FIGURE 8: Phenylalanine ν_{12} Raman cross sections with 229-nm excitation, as a function of the ethylene glycol content of the aqueous solutions.

SUMMARY

(1) The strength of tyrosine H-bond interactions in proteins can be assessed from the frequency of the ring mode ν_{8b} for which optimum selectivity is obtained with 229-nm excitation. For the ovomucoid and purothionin proteins, strong H-bonds are readily detectable, with estimated $-\Delta H$ values of 10–14 kcal/mol.

(2) The tyrosine Fermi doublet UVRR intensity ratio can be used as an indicator of H-bond changes for a given Tyr residue, but quantitative evaluation is made problematic by additional environmental effects, as illustrated by the purothionins. If the H-bond strength is known from ν_{8b}, then the Fermi doublet can be used as a marker of these additional effects.

(3) The UVRR intensity of the Tyr ring mode ν_{9a} also depends strongly on H-bonding, but again there are additional environmental effects.

(4) Environmental effects on aromatic ring mode RR intensities are expected to be the rule, as illustrated by the changes in the Phe ν_{12} band intensity observed on ethylene glycol addition, which mimic the increased cross sections seen in proteins.

ACKNOWLEDGMENTS

We thank J. Perno and R. Czernuszewicz for expert assistance.

REFERENCES

Arnett, E. M., Jorres, C., Mitchell, E., Murty, T. S. S. R., Gorrie, T. M., & von Schleyer, R. P. (1970) *J. Am. Chem. Soc. 92*, 2365.

Asher, S. A., Ludwig, M., & Johnson, C. R. (1986) *J. Am. Chem. Soc. 108*, 3186.

Baker, E. N., & Hubbard, R. E. (1984) *Prog. Biophys. Mol. Biol. 44*, 97.

Bellocq, A. M., Lord, R. C., & Mendelsohn, R. (1972) *Biochim. Biophys. Acta 257*, 280.

Bode, W., Epp, O., Huber, R., Laskowski, M., Jr., & Ardelt, W. (1985) *Eur. J. Biochem. 147*, 387.

Cantor, C. R., & Schimmel, P. R. (1980a) in *Biophysical Chemistry*, Part I, pp 41–154, W. H. Freeman, New York.

Cantor, C. R., & Schimmel, P. R. (1980b) in *Biophysical Chemistry*, Part II, pp 349–408, W. H. Freeman, New York.

Chinsky, L., Jolles, B., Laigle, A., & Turpin, P. Y. (1985) *J. Raman Spectrosc. 16*, 235.

Copeland, R. A., & Spiro, T. G. (1985) *Biochemistry 24*, 4960.

Copeland, R. A., & Spiro, T. G. (1986) *J. Am. Chem. Soc. 108*, 1281.

Copeland, R. A., & Spiro, T. G. (1987) *Biochemistry, 26*, 2134.

Copeland, R. A., Dasgupta, S., & Spiro, T. G. (1985) *J. Am. Chem. Soc. 107*, 3370.

Creighton, T. E. (1983) in *Proteins, Structure and Molecular Properties* pp 133–158, W. H. Freeman, New York.

Demchenko, A. P. (1986) *Ultraviolet Spectroscopy of Proteins*, Springer-Verlag, Berlin, West Germany.

Dollish, F. R., Fately, W. G., & Bentley, F. F. (1974) *Characteristic Raman Frequencies of Organic Compounds*, p 162ff, Wiley, New York.

Donovan, J. W. (1973) *Methods Enzymol., Part D, 27*, 497.

Dunken, H., & Fritzsche, H. (1961) *Z. Chem. 1*, 249.

Eploy, T. D., & Drago, R. S. (1967) *J. Am. Chem. Soc. 89*, 5770.

Farak, L., Giles, G., Wilson, D., Ohno, A., & Scott, R. M. (1979) *J. Phys. Chem. 83*, 2455.

Fersht, A. R., Shi, J.-P., Knill-Jones, J., Lowe, D. M., Wilkinson, A. J., Blow, D. M., Brick, P., Carter, P., Waye, M. M. Y., & Winter, G. (1985) *Nature (London) 314*, 235.

Fodor, S. P. A., Rava, R. P., Copeland, R. A., & Spiro, T. G. (1986) *J. Raman Spectrosc. 17*, 471.

Fodor, S. P. A., Copeland, R. A., & Spiro, T. G. (1987) *J. Am. Chem. Soc.* (in press).

Fritzsche, H. (1964) *Ber. Bunsen-Ges. Phys. Chem. 68*, 459.

Gramstad, T. (1961) *Acta Chem. Scand. 16*, 807.

Gramstad, T. (1963) *Spectrochim. Acta 19*, 497.

Harada, I., & Tachenki, H. (1986) in *Spectroscopy of Biological Systems* (Clark, R. J. H., & Hester, R. E., Eds.) Chapter 3, Wiley, New York.

Harada, I., Takamatsu, T., Slumanouchi, T., Miyazawa, T., & Tamiya, N. (1976) *J. Phys. Chem. 80*, 1153.

Hendrickson, W. A., & Teeter, M. M. (1981) *Nature (London) 290*, 107.

Hudson, B., & Mayne, L. (1984) *Methods Enzymol. 130*, 331.

Joesten, M. D., & Drago, R. S. (1962) *J. Am. Chem. Soc. 84*, 2696.

Joesten, M. D., & Schaad, L. J. (1974) *Hydrogen Bonding*, p 2, M. Dekker, New York.

Johnson, C. R., Ludwig, M., O'Donnell, S., & Asher, S. A. (1984) *J. Am. Chem. Soc. 106*, 5008.

Jones, B. L., & Mak, A. S. (1977) *Cereal Chem. 54*, 511.

Kato, I., Schrode, Y., Kohr, W. Y., & Laskowski (1987) *Biochemistry 26*, 193.

Kogowski, G., Scott, R. M., & Filisko, F. (1980) *J. Phys. Chem. 84*, 2262.

Laskowski, M., Jr., & Kato, I. (1980) *Annu. Rev. Biochem. 49*, 593.

Laskowski, M., Jr., Kato, I., Ardelt, W., Cook, J., Denton, A., Empie, M. W., Kohr, W. J., Park, S. J., Parks, K., Schatzley, B. L., Schoenberger, O. L., Tashiro, M., Vichot, G., Whatley, H. E., Wieczorek, A., & Wieczorek, M. (1987) *Biochemistry 26*, 202.

Lecomte, J. T. J., Jones, B. L., & Llinas, M. (1982) *Biochemistry 21*, 4843.

Mak, A. S. (1975) Ph.D. Thesis, University of Manitoba, Winnipeg, Manitoba, Canada.

Mak, A. S., & Jones, B. L. (1976) *Can. J. Biochem. 22*, 835.

McHale, J. L. (1982) *J. Raman Spectrosc. 13*, 21.

Neerinck, D., van Audenhaege, A., & Lamberts, L. (1969) *Ann. Chim. 14*, 43.

Papamokos, E., Weber, E., Bode, W., Huber, R., Empie, M. W., Kato, I., & Laskowski, M., Jr. (1982) *J. Mol. Biol. 158*, 515.

Prendergast, F. G., Hampton, P. D., & Jones, B. (1984) *Biochemistry 23*, 6690.
Rava, R. P., & Spiro, T. G. (1984) *J. Am. Chem. Soc. 106*, 4062.
Rava, R. P., & Spiro, T. G. (1985a) *Biochemistry 24*, 1861.
Rava, R. P., & Spiro, T. G. (1985b) *J. Phys. Chem. 89*, 1856.
Sherry, A. D. (1976) in *The Hydrogen Bond* (Schuster, P., Zundel, G., & Sandorfy, C., Eds.) Vol. III, Chapter 25, North-Holland, Amsterdam, The Netherlands.
Siamwiza, M. N., Lord, R. C., Chen, M. C., Takamatsu, T., Harada, I., Matsuura, H., & Shimanouchi, T. (1975) *Biochemistry 14*, 4870.
Singh, S., & Rao, C. N. R. (1966) *Can. J. Chem. 44*, 2611.
Singh, S., Murthy, A. S. N., & Rao, C. N. R. (1966) *Trans. Faraday Soc. 62*, 1056.
Teeter, M. M., & Hendrickson, W. A. (1979) *J. Mol. Biol. 127*, 219.
Thijs, R., & Zeegers-Huyskens, Th. (1984) *Spectrochim. Acta, Part A 40A*, 1057.
Tu, A. T. V. (1986) *Adv. Spectrosc. (Chichester, U.K.) 13*, 47.
Vogel, G. C., & Drago, R. S. (1970) *J. Am. Chem. Soc. 92*, 5397.
Walsh, C. (1979) in *Enzyme Reaction Mechanisms*, W. H. Freeman, New York.
Walters, A. M., Scholler, D. M., Hoffman, B. M., & Spiro, T. G. (1983) *J. Raman Spectrosc. 14*, 162.
Weber, E., Papamokos, E., Bode, W., Huber, R., Kato, I., & Laskowski, M., Jr. (1981) *J. Mol. Biol. 149*, 109.
Weiner, S. J., Kollman, P. A., Case, D. A., Singh, U. C., Ghio, C., Alagona, G., Profeta, S., Jr., & Weiner, P. (1984) *J. Am. Chem. Soc. 106*, 765.
West, R., Powell, D. L., Lee, M. K. T., & Watley, L. S. (1964) *J. Am. Chem. Soc. 86*, 3227.
Williams, R. W., & Teeter, M. M. (1984) *Biochemistry 23*, 6796.
Yu, N. T., Jo, B. H., & O'Shea, D. C. (1973) *Arch. Biochem. Biophys. 156*, 171.
Zharkov, V. V., Zhitinkina, A. V., & Zkokhova, F. A. (1970) *Zh. Fiz. Khim. 44*, 223.
Ziegler, L. D., & Hudson, B. (1981) *J. Chem. Phys. 74*, 982.
Ziegler, L. D., & Hudson, B. (1983) *J. Chem. Phys. 79*, 1134.

A Comparison of the Resonance Raman Properties of the Fast and Slow Forms of Cytochrome Oxidase†

Jon R. Schoonover,‡,§ R. Brian Dyer,‡ William H. Woodruff,*,‡ Gary M. Baker,§ Masato Noguchi,§ and Graham Palmer*,§

Isotope and Structural Chemistry Group (INC-4), Los Alamos National Laboratory, University of California, Mail Stop C346, Los Alamos, New Mexico 87545, and Department of Biochemistry, Rice University, P.O. Box 1892, Houston, Texas 77251

Received October 14, 1987; Revised Manuscript Received February 11, 1988

ABSTRACT: Resonance Raman (RR) spectra of the "rapid" and "slow" forms (Baker et al., 1987) of resting cytochrome oxidase obtained with Soret excitation at 413.1 nm are reported. There are a number of conspicuous differences between the two forms in the high-frequency region of the RR spectrum which involve changes in Raman intensity arising from a blue shift in the Soret maximum of cytochrome a_3 upon conversion to the slow form. In the low-frequency region a peak present at 223 cm^{-1} in the rapid form shifts to 220 cm^{-1} in the slow form; this peak is assigned as the cytochrome a_3 Fe(III)–N(His-Im) stretch. The slow form of the enzyme possesses greater intensity in RR peaks near 1620 cm^{-1} which have been previously attributed by others to partial photoreduction of the enzyme. We have quantitated the amount of laser-induced photoreduction in these RR spectra by comparison with the spectra of mixed-valence derivatives of the enzyme and find that these 1620-cm^{-1} features are unreliable indicators of photoreduction. The spectra of the fast- and slow-reacting species in H_2O and D_2O have been compared. The fast-reacting form exhibits a 4-cm^{-1} shift, from 223 to 219 cm^{-1}, upon transferring to D_2O in a peak which we assign as the cytochrome a_3 Fe(III)–N(His-Im) stretch. There is a parallel shift in the feature at 1651 cm^{-1} due to the C=O stretch of the formyl group of cytochrome *a*. These deuterium shifts are not observed in the slow form. We suggest that the nature of the difference between the fast and slow forms of the enzyme is a global conformational change involving inter alia the axial histidine ligand of cytochrome a_3 and the cytochrome *a* environment. This conformational change is also responsible for the enhanced Raman intensity observed at 1620 cm^{-1} in the slow form. Some mechanisms whereby such a conformational change might affect the cytochrome a_3 Soret energy are discussed.

Cytochrome oxidase catalyzes the four-electron reduction of dioxygen to water and accepts the required electrons from the cellular respiratory chain via cytochrome *c*. The enzyme also conserves the energy of the cytochrome *c*–O_2 redox couple (~500 mV) by consuming four protons in the mitochondrial matrix space and by active pumping of additional protons to the cytosolic space. This creates a transmembrane ion gradient which is used to drive the synthesis of adenosine 5′-triphosphate (ATP) (Malmström, 1979; Wikström et al., 1981).

Electron paramagnetic resonance (EPR), magnetic circular dichroism (MCD), and magnetic susceptibility measurements have provided information on the electronic structure of the

† This investigation was supported by National Institutes of Health Grants DK 36263 (W.H.W.) and GM 21337 (G.P.) and Robert A. Welch Foundation Grant C-636 (G.P.). Portions of this work were performed at Los Alamos National Laboratory under the Auspices of the U.S. Department of Energy.

* Address correspondence to this author.
‡ Los Alamos National Laboratory.
§ Rice University.

0006-2960/88/0427-5433$01.50/0